



ROE (Radiotherapy Outcomes Estimator): An open-source tool for optimizing radiotherapy prescriptions



Aditi Iyer ^{a,*}, Aditya P. Apte ^a, Ethan Bendau ^b, Maria Thor ^a, Ishita Chen ^c, Jacob Shin ^d, Abraham Wu ^d, Daniel Gomez ^d, Andreas Rimner ^d, Ellen Yorke ^a, Joseph O. Deasy ^a, Andrew Jackson ^a

^a Department of Medical Physics, Memorial Sloan Kettering Cancer Center, 1275 York Ave, New York, NY, United States

^b Department of Biomedical Engineering, Columbia University, New York, NY, United States

^c Department of Radiation Oncology, Tennessee Oncology, Nashville, TN, United States

^d Department of Radiation Oncology, Memorial Sloan Kettering Cancer Center, New York, NY, United States

ARTICLE INFO

Keywords:

Radiotherapy outcome modeling
Prescription determination
Tumor control probability
Normal tissue complication probability
Radiotherapy analysis software

ABSTRACT

Background and objectives: Radiotherapy prescriptions currently derive from population-wide guidelines established through large clinical trials. We provide an open-source software tool for patient-specific prescription determination using personalized dose-response curves.

Methods: We developed ROE, a plugin to the Computational Environment for Radiotherapy Research to visualize predicted tumor control and normal tissue complication simultaneously, as a function of prescription dose. ROE can be used natively with MATLAB and is additionally made accessible in GNU Octave and Python, eliminating the need for commercial licenses. It provides a curated library of published and validated predictive models and incorporates clinical restrictions on normal tissue outcomes. ROE additionally provides batch-mode tools to evaluate and select among different fractionation schemes and analyze radiotherapy outcomes across patient cohorts.

Conclusion: ROE is an open-source, GPL-copyrighted tool for interactive exploration of the dose-response relationship to aid in radiotherapy planning. We demonstrate its potential clinical relevance in (1) improving patient awareness by quantifying the risks and benefits of a given treatment protocol (2) assessing the potential for dose escalation across patient cohorts and (3) estimating accrual rates of new protocols.

1. Introduction

Radiation therapy (RT) is an important and cost-effective treatment modality, contributing to curative treatment in 40% of all cancer patients [1]. The success of RT relies on balancing two competing factors: maximizing the radiation dose delivered to cancer cells and restricting the dose to the surrounding normal tissue, to minimize undesired complications.

Currently, RT prescriptions are largely population-based, deriving from outcomes of large clinical trials [2]. Personalizing prescriptions by taking into account predicted tumor control probability (TCP) and

normal tissue complication probability (NTCP) could yield more favorable trade-offs and help identify patients for dose intensification or de-escalation.

Few software tools exist for treatment planning informed by predicted RT outcomes [3–5]. Those available typically do not present NTCP and TCP jointly as a function of prescription dose. Further, incorporation of NTCP and TCP models into routine treatment planning systems has been limited by narrow libraries of integrated models, and restrictions on custom (user-defined) models and combining NTCP and dose-volume histogram (DVH) based constraints. They also lack batch-mode tools for protocol development and planning quality

* Corresponding author.

E-mail address: iyera@mskcc.org (A. Iyer).

assurance based on NTCP and TCP. We developed an open-source tool, ROE (Radiotherapy Outcomes Estimator), to address these limitations and aid in exploring the impact of RT prescriptions on patient outcomes. In designing this tool, we took into consideration the recommendations of the AAPM therapy physics committee [6]. ROE provides five of the six features identified in the report: (1) ability to select from a curated library of model parameters and modify input values (2) supporting both NTCP and DVH-based constraints (3) ability to input dose-modifying parameters (e.g. biological factors or pre-existing conditions) (4) ability to maximize TCP while respecting a given NTCP limit or minimize NTCP while achieving a specified TCP and (5) supporting user-defined stop-values on NTCP and DVH metrics.

ROE is designed as a plugin to the Computational Environment for Radiological Research (CERR) [7], leveraging its existing capabilities for data import, management, and processing. It is available for download as a CERR module at <https://github.com/cerr/CERR.git>. ROE aims to facilitate (1) patient-specific prescription optimization by scaling fraction size or fraction number and (2) fractionation selection in individual patients or cohorts as demonstrated in [8], either by comparing the maximum achievable TCP/BED while respecting NTCP constraints or comparing levels of NTCP at required values of TCP across different fractionation schemes. We recommend that scaled dose distributions suggested by ROE be independently evaluated within the treatment planning system to ensure validity and deliverability.

2. Architecture

ROE provides a graphical interface (Fig. 1) for interactive exploration of RT dose-response relationships. It has been developed as a MATLAB-based plugin to CERR. Flexible JSON-format [9] files are used to input dose fractionations, model parameters, and clinical constraints. Several pre-defined and validated models (TCP, BED, and NTCP) are included in the distribution. ROE requires an input treatment plan and one or more associated fractionation schemes, which scale the existing plan up or down. Fractionation schemes can be compared across a cohort using the batch mode tool CoROE (Cohort ROE).

2.1. Dose-volume factors

DICOM-RT objects including structures, plans, and dose objects are imported to CERR-format archives for simplified access to treatment planning information. ROE extracts 3D dose distributions and structure masks, which are then summarized in the form of DVHs. These and related metrics needed to estimate TCP and NTCP are computed using previously validated CERR routines.

2.2. Predictive models

Modules describing functional forms commonly used in NTCP

Table 1

Dosimetric models available in ROE.

Functional form	Models	Internal validation	Site
Conventional			
Linear	Erectile dysfunction [12]	-	Prostate
Logistic	Dysphagia [13], Esophagitis [14,15], Lung tumor control [16]	Yes [18]	Head and neck Lung
LKB	Pulmonary toxicity [17] Rectal bleeding [20], Late urinary toxicity [21, 22], Radiation-induced liver disease [23]	Yes [19]	Lung Prostate Gastrointestinal
Cox	Cardiopulmonary toxicity [24]	-	Lung
Biexponential	Xerostomia [25]	-	Head and neck
Fowler BED [26]	Lung tumor BED [27]	-	Lung
Advanced			
Mechanistic 1	Lung tumor control [28]	-	Lung
Mechanistic 2	Prostate tumor control [29]	-	Prostate
Appelt modification	Radiation pneumonitis [30]	Yes [18]	Lung
Chest-wall pain	Chest-wall pain [31]	-	Lung

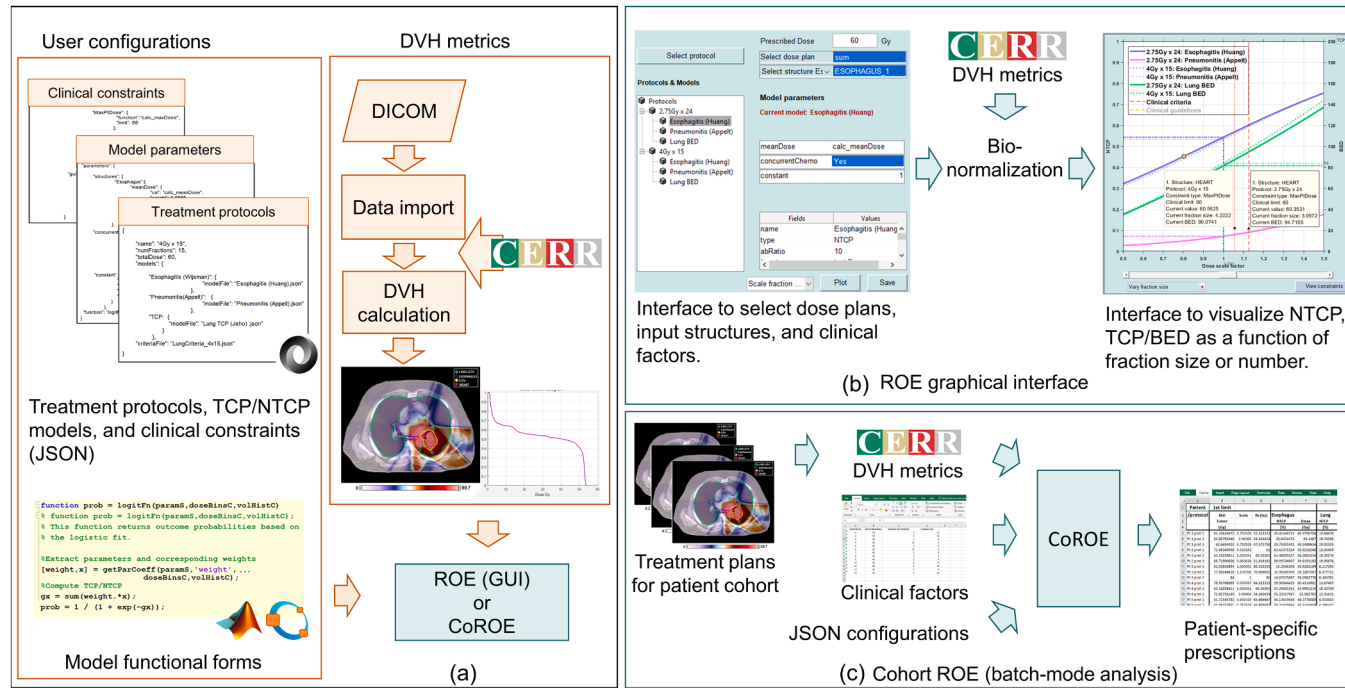


Fig. 1. Components of the Radiotherapy Outcomes Estimator: (a) Inputs: user-specified models, clinical constraints on normal tissues, and treatment plans (b) Graphical interface showing dose-response curves and (c) CoROE: batch-mode extension for analyzing patient cohorts.

modeling, such as the Lyman Kutcher Burman (LKB) [10], linear, logistic, and Cox proportional hazards [11] are distributed with ROE. Non-standard functional forms for selected TCP and NTCP models are also provided. All models currently distributed with ROE are presented in Table 1. These implementations have been verified against manual calculations using single and multi-voxel structures for whole and inhomogeneous dose-volume responses, and a unit test suite is provided to ensure ongoing validity.

ROE also supports custom-definition of model forms via MATLAB functions with the signature:

```
outcome = functionName(paramS, doseBinsV, volBinsV)
```

where ‘paramS’ is a MATLAB/GNU Octave “structure” data type (equivalent to Python’s “dictionary” data type) containing parameter names and associated values, ‘doseBinsV’ and ‘volBinsV’ represent dose-histogram bins and corresponding volumes input as vectors (single-structure models) or cell arrays (multi-structure models).

To apply published models distributed with ROE (Table 1), the input dose is bio-normalized to match the original modeled dataset. Using the linear quadratic model [32], physical dose histogram bins are translated to biologically equivalent doses delivered in the fraction number or size cited in the modeled dataset (see Appendix A.1 for further details). Coefficients and parameters for individual models can be found in the respective publications cited in the table.

2.3. Configuring fractionation schemes, model parameters, and clinical constraints

JSON files follow a predefined syntax to specify fractionation schemes, model parameters, and clinical constraints. This format supports human-readable, structured data input, making it easy to define sophisticated models using key-value pairs and ordered lists.

Fractionation schemes are specified in terms of prescribed dose and number of fractions. Models are specified through their functional forms, predictors and coefficients, and list of applicable tumors or critical structures. Predictors can include multivariate clinical risk factors (age, gender, stage etc.) as well as DVH-based metrics. Predefined configurations for selected models across different sites (head and neck, lung, prostate) are distributed with ROE. Some of these models have been validated against data from our institution for calibration and predictive power (indicated in Table 1). However, this is not a requirement for use with ROE. Future additions to ROE’s library of models will be documented at [https://github.com/cerr/CERR/wiki/Radiotherapy-Outcomes-Estimator-\(ROE\)-](https://github.com/cerr/CERR/wiki/Radiotherapy-Outcomes-Estimator-(ROE)-) and available for download along with CERR.

Clinically-used NTCP and dose-volume based constraints are specified as limits (always operational) or guidelines (contingent on target coverage) through JSON files. These files list NTCP or DVH metrics and associated limits, along with CERR (or user-defined) functions for their evaluation. Sample JSON configurations for fractionation schemes, model parameters, and clinical constraints, are accessible at https://github.com/cerr/CERR/tree/master/CERR_core/PlanAnalysis/sampleFilesForROE/.

2.4. Octave and Python compatibility

ROE’s source code is compatible with GNU-Octave, eliminating the need for commercial licenses. It is accessible via Python using the bridge library Oct2py, which handles datatype conversions between Octave and Python. This allows for cloud-based access to ROE tools via Jupyter notebooks. A sample notebook demonstrating ROE functionality on the Google Colab platform is distributed at https://github.com/stratis-forge/roe-workflows/blob/main/demo_ROE_normal_tissue_and_tumor_response_curves.ipynb

3. Features

3.1. Visualization modes

ROE supports two modes of optimizing prescriptions: using a fixed fraction number (modifying the dose per fraction) or a fixed fraction size (modifying the fraction number), while respecting clinical constraints. Two additional visualization modes (detailed in Section 3.1.3) provide different ways of representing the impact on TCP/BED and NTCP simultaneously.

A relative dose distribution is constructed from the input dose distribution divided by the input prescription, which is then rescaled to simulate the user-input fractionation. DVHs for all structures of interest are then extracted and processed depending on the selected mode.

3.1.1. Scaling fraction size

To simulate a variety of fraction sizes, dose histogram bins from the baseline fractionation (at scale factor=1) are scaled by 100 equally-spaced multiplicative factors in a user-input range (by default, [0.5–1.5]). This is followed by bio-normalization as outlined in Section 2.2. Models are evaluated at each scale factor, producing dose-response (NTCP and TCP/BED) curves as a function of fraction size. This display mode enables patient-specific tailoring of fraction size while respecting normal tissue constraints (Fig. 2(a)).

3.1.2. Scaling fraction number

Beginning with baseline fraction number N and constant fraction size, dose histogram bins are scaled by factors $\frac{N + \Delta N}{N}$ to simulate a range of fraction numbers. Schemes considered include ΔN in $[-N_{max}, N_{max}]$ where N_{max} is the nearest integer to $(N/2)$. This is followed by bio-normalization as outlined in Section 2.2. Models are evaluated at each scale factor, producing dose-response curves (NTCP and TCP/BED) as a function of fraction number. This display mode facilitates the selection of the optimal fraction number without exceeding normal tissue limits (Fig. 2(b)).

3.1.3. NTCP vs. TCP and NTCP vs. BED

These modes summarize the various effects on tumor and normal structures into a single, simplified curve for each normal tissue, facilitating the selection of a new fractionation scheme at a glance. NTCP is plotted as a function of either TCP or BED as selected, and the underlying algorithm is identical to scaling the fraction number. In this mode, tool-tips show the fraction number and prescription dose at the first limiting value of NTCP encountered (Fig. 2(c)).

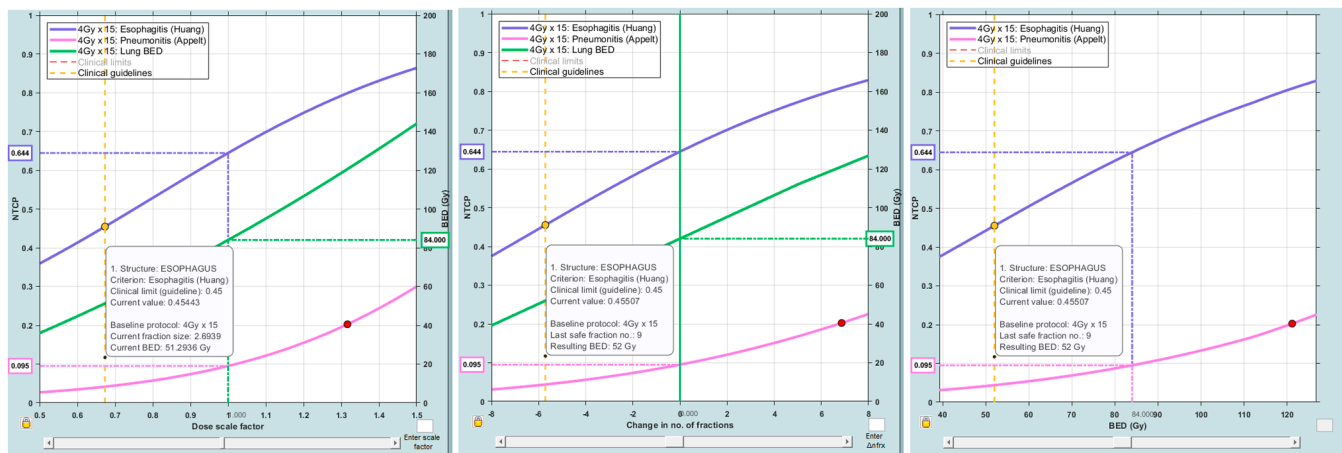


Fig. 2. Evaluating the 4 Gy x 15 baseline fractionation applied to a patient with non-small cell lung cancer (NSCLC) using different visualization modes: (a) NTCP and BED as function of fraction size (b) NTCP and BED as function of fraction number and (c) NTCP vs. BED (at a range of fraction numbers). The interface displays the first constraint (limit or guideline) encountered by default in all visualization modes.

3.2. Display of clinical criteria

Violation markers on the NTCP curves indicate the lowest fraction size or number causing a breach of the user-supplied clinical constraints (guidelines marked yellow and limits in red). Additionally, fractionation schemes resulting in violations of dose-volume based constraints are indicated by vertical lines. The first operative constraint for each fractionation scheme is displayed by default, with guideline violations in yellow and limits in red. A secondary ‘Constraints’ tab, listing all available constraints (NTCP and DVH-based), is provided for interactive display (Fig. 3). Users can selectively display or disable each constraint, or cycle through them sequentially in their order of violation. Expandable tool-tips summarize information pertaining to constraint violations such as violated metrics and clinically desirable values, suggested modifications to fraction size or number, and resulting tumor TCP/BED.

3.3. CoROE: batch-mode analysis

Batch-mode tools are provided to facilitate fractionation comparison and selection across a cohort. Dose distributions and segmentation masks are extracted from CERR archives following harmonization of structure names. CERR provides a renaming tool to facilitate this, documented on ROE’s Wiki page ([https://github.com/cerr/CERR/wiki/Radiotherapy-Outcomes-Estimator-\(ROE\)](https://github.com/cerr/CERR/wiki/Radiotherapy-Outcomes-Estimator-(ROE))). Relevant clinical factors (age, gender etc.) and treated doses are input through spreadsheets; fractionation schemes, models (TCP/BED and NTCP), and clinical constraints are input through JSON-format files as described in Section 2.3.

3.3.1. Fractionation comparison by scaling fraction size

Input dose distributions are scaled to match the selected fractionations. Keeping fraction numbers fixed, complication rates for normal structures are estimated over a range of fraction sizes, simulated by scaling the baseline value between a user-input range of factors (by

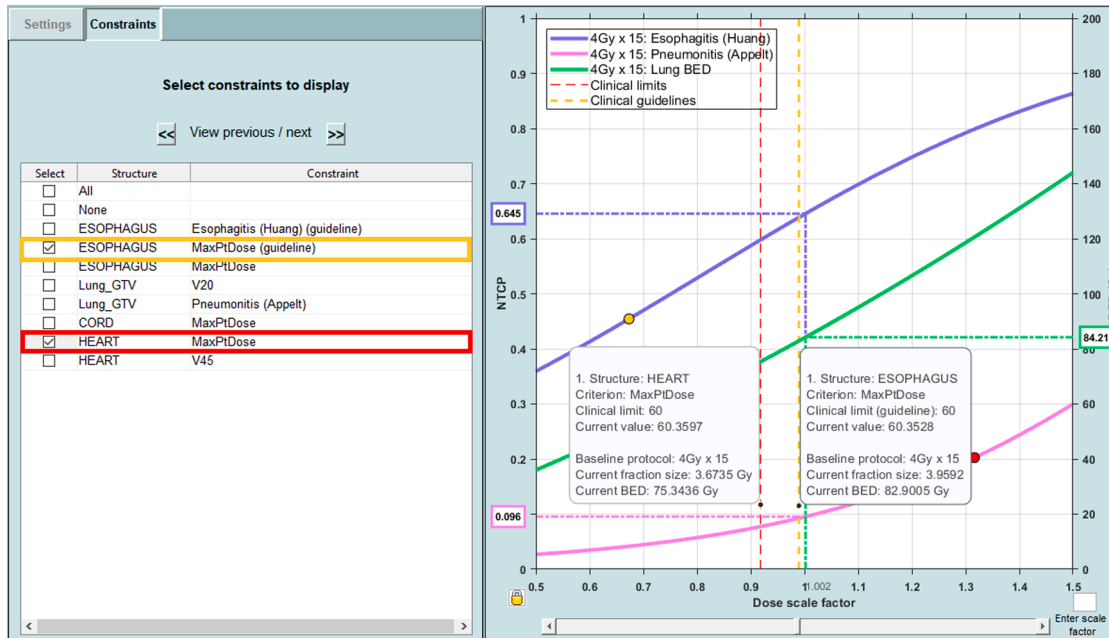


Fig. 3. ROE interface showing dose responses for a NSCLC patient treated with 4 Gy x 15. NTCP violation markers for esophagitis (45 % guideline in yellow) and pneumonitis (20 % limit in red) are indicated by default. Violations of dose-volume constraints selected by the user: maximum doses to the esophagus (yellow guideline) and heart (red limit) are additionally displayed.

default, [0.5,1.5]). User-specified dose-volume metrics are evaluated over the same range. The smallest scale factor resulting in violation of clinical constraints on each clinical NTCP/dose-volume constraint is recorded. Clinical guidelines are only considered on dose escalation (i.e., scale factors >1), whereas limits are always operational. The first of these violations is identified, and all NTCP, dose-volume metrics, and TCP/BED are recorded at the corresponding scale factor. In some cases, the first constraint may be too restrictive to achieve acceptable TCP. Therefore, relevant metrics are additionally recorded at the scale factor producing the second violation. Results of this analysis are summarized in a spreadsheet, identifying the suggested fractionation, constraining

factors, and clinically relevant NTCP/DVH metrics for each patient. This tool could be applied to retrospective evaluation of patient cohorts for protocol comparison and selection, as well as prospective validation of treated protocols.

3.3.2. Achieving target TCP or BED by scaling fraction size

In some patients, the maximum achievable TCP/BED is severely restricted by clinical dose-volume constraints on normal tissues. COROE provides tools for fractionation selection in such cases by scaling fraction sizes to achieve either acceptable TCP or BED. Input dose distributions are scaled to match the selected fractionations. Keeping fraction

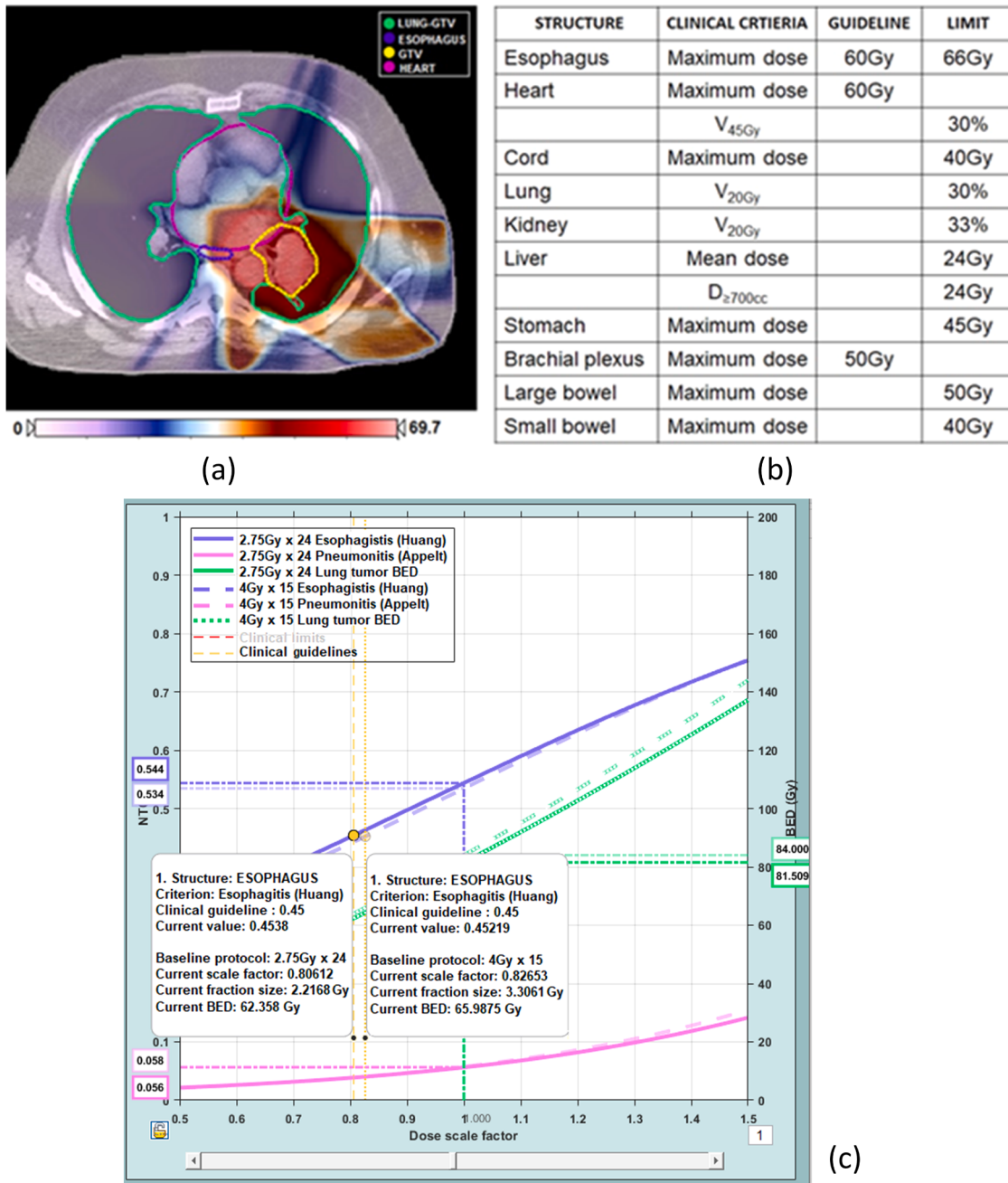


Fig. 4. (a) Treatment plan with prescribed dose of 66 Gy showing GTV, lung (excluding GTV), esophagus, and heart contours visualized in CERR. (b) Relevant clinical criteria (c) Comparison of two fractionation schemes in ROE, P1: 2.75 Gy x 24 and P2: 4 Gy x 15. The tooltip displays the first normal tissue constraint violated (here, the Esophagitis NTCP from the Huang et al. model [14]), clinical tolerance (labeled "Clinical guideline: 0.45") and the value at the first violation ("Current value: 0.4538" under P1 and "Current value: 0.45219" under P2). It also indicates the limiting fraction size ("Current fraction size: 2.2168Gy" under P1 and "Current fraction size: 3.3061Gy" under P2) and associated BED ("Current BED: 62.358 Gy" under P1 and "Current BED: 65.9875 Gy" under P2). The user may accept the suggested BED or override normal tissue constraints to escalate the dose until the next violation occurs.

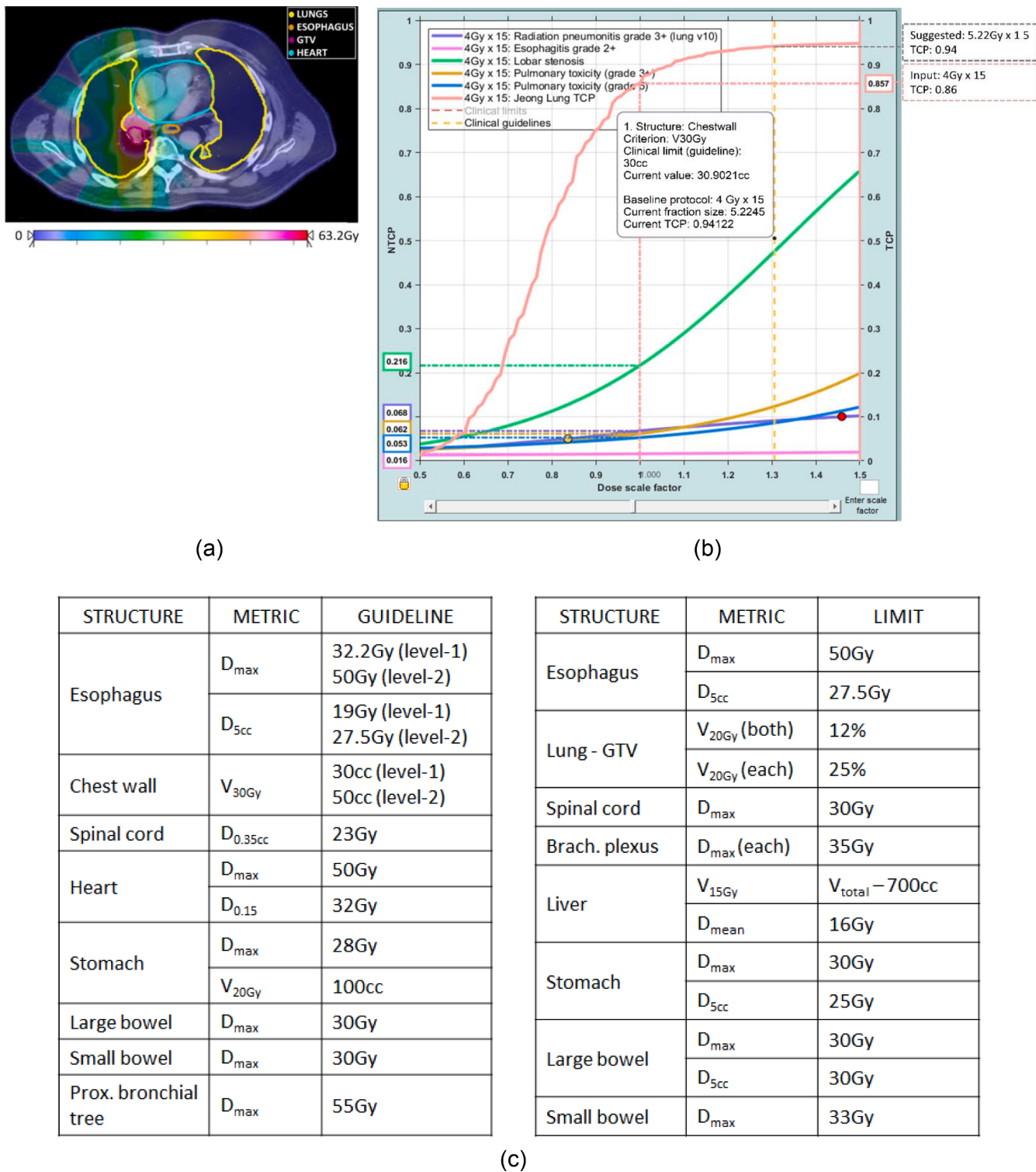


Fig. 5. (a) Treatment plan with prescribed dose of 60 Gy showing GTV, lung (excluding GTV), esophagus, and heart. (b) Improvement in predicted TCP using personalized Rx=78.3 Gy vs. original Rx=60 Gy. (c) List of clinical criteria considered.

numbers fixed, TCP is estimated over a variety of fraction sizes, simulated by scaling the baseline value over a user-input range (by default, [0.5,1.5]). The lowest scale factor that meets the user-specified TCP (or BED) threshold is identified. Results of this analysis are summarized in a spreadsheet specifying the fraction size required to achieve acceptable TCP/BED, corresponding normal tissue metrics, and identifying constraint violations.

4. Applications

The following sections illustrate several use cases of ROE as applied to NSCLC.

4.1. Comparison of fractionation schemes for a single patient

We considered two baseline fractionations for treating NSCLC: 66 Gy

in 24 fractions and 60 Gy in 15 fractions, using ROE to identify the maximum achievable tumor BED in each case by modifying fraction size (Fig. 4). A limit of 20 % was imposed on grade 3+ radiation pneumonitis (RP) rates estimated using the Appelt et al. model [30], and a 45 % guideline was adopted for grade 2+ acute esophagitis (AE) rates estimated using the Huang et al. model [14]. Tumor BED was estimated using the Fowler's model [26] including corrections for repopulation with appropriate parameters for lung cancer from [27]. Patient risk factors including lower/middle tumor location and former smoking status were input through the interface and dose-volume constraints listed in Fig. 4(b) were input via JSON.

At 24 fractions, the first constraint violation was observed at fraction size 2.21 Gy due to predicted AE rate > 45 %, with the tumor BED being 62.06 Gy. A higher tumor BED of 65.66 Gy was achievable with treatment in 15 fractions at a fraction size of 3.29 Gy, beyond which, the predicted AE rate exceeded 45 %.

4.2. Prescription determination for treatment planning of a single patient

We rescaled an ECHO [33]-optimized treatment plan (60 Gy in 15 fractions) for a patient with ultracentral NSCLC using ROE. NTCP model-based limits on grade 2+ AE (30 %) and grade 3+ RP (10 %) were enforced, along with dose-volume guidelines and limits listed in Fig. 5(c). Guidelines were only considered on escalating dose, i.e., for Rx > 60 Gy. TCP was estimated using [28]. The rescaled prescription of 78.3 Gy in 15 fractions yielded a predicted TCP of 94 %, a 9 % improvement over the predicted TCP for the original prescription (Fig. 5(b)). This demonstrates the potential for patient-specific prescription selection using ROE to maximize TCP while respecting clinical constraints.

4.3. Comparison of proposed fractionations using plans from a previously treated cohort

We used CoROE to evaluate the potential for dose escalation in treatment plans of 241 Stage-III NSCLC patients previously treated with intensity modulated RT (IMRT) and concurrent or sequential chemotherapy. Multivariate dose-response models were used to predict grade 2+ AE2 [14]; RP [30]; and prescription-based tumor BED [27]. Dose-volume metrics, adjusted using the linear-quadratic model [32], were compared with existing clinical limits for 4 Gy X 15 treatments. Prescription was optimized over fraction size and fraction number, by scaling the fraction size for each fraction number (scale: 0.5–1.5), with 4 Gy X 15 as baseline. At each fraction number, all tumor/normal tissue metrics were recorded after the first dose-limiting normal tissue constraint was encountered, and the prescription achieving the highest tumor BED was selected. The models estimated that 71% of patients

could be treated to doses > 62.7 Gy (equivalent to a physical prescription of 60 Gy in 2 Gy fractions) (Fig. 6(a)). All but one patient with tumor BEDs < 62.7 Gy were limited by lung constraints (Fig. 6(b)), either V20 < 30 % or Lung NTCP < 20 %. Patients with tumor BEDs > 84 Gy were limited by constraints on the maximum dose to the esophagus (< 60 Gy in 15 fractions unless tumor BED < 84 Gy, < 66 Gy in 15 fractions otherwise) in 54 patients, and/or heart (< 60 Gy in 15 fractions unless tumor BED < 84 Gy) in 46 patients.

CoROE predicted that dose-escalation was possible in the majority of NSCLC patients and identified those patients for whom treatment to potentially curative doses would place them at high risk for complications. This demonstrates the potential for assisting physicians in patient-specific selection of treatment prescriptions.

4.4. Estimating the eligible number of patients for RT protocols using dose-volume guidelines

RT protocols accruing patients more slowly than expected risk being closed. Accrual rates depend, among other things, on the number of eligible patients. CoROE's functionality for evaluating dose-volume metrics in patient cohorts can be leveraged to estimate the accrueable proportion of patients for new in-house protocols.

We considered a protocol proposed to test the efficacy of a drug treatment for esophagitis following RT for thoracic tumors utilizing various prescriptions (Table 2). Patients were deemed eligible at the time of treatment planning if, using dose-volume criteria based on [14],

Table 2

CoROE estimates of numbers of eligible patients for proposed RT protocol at various prescriptions.

Cohort	Protocol	Esophagus constraint	Avg #pts per year	Estimated% eligible	Estimated #eligible pts/year
C1	3 Gy x 10	V30>15 %	94	6.56	6.16
	3 Gy x 15	V40>15 %	135.5	50.8	68.9
	2.75 Gy x 20	V40>15 %	53.5	68.9	36.8
	1.8 Gy x 25	V50>5 %	33	0	0
	1.8 Gy x 28	V50>5 %	133.5	9.84	13.1
	1.8 Gy x 30	V50>5 %	85	45.9	39
	2 Gy x 30	V50>5 %	162	54.1	87.6
	2 Gy x 33	V50>5 %	19	65.6	12.5
	2 Gy x 35	V50>5 %	6	70.5	4.23
	4 Gy x 15	V40>15 %	43.5	9.524	4.14
Total					272.4

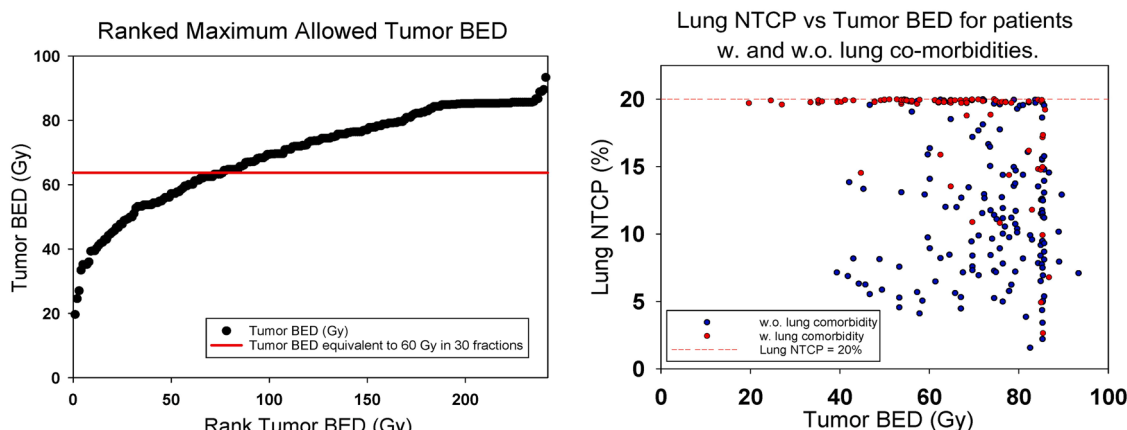


Fig. 6. (a) CoROE predicted tumor BED < 62.7 Gy in 71 patients, 30 of whom had predicted BED < 50 Gy. (b) Patients with lung comorbidities (red dots) were determined to be limited primarily by lung NTCP, in contrast to patients without (blue dots).

[15,34], they were at high risk for AE. CoROE was used to estimate the eligible proportion of 235 late-stage NSCLC patients (cohort C1) receiving 50–80 (median:66) Gy in 1.8–2 Gy fractions using chemotherapy combined with IMRT from 2004 to 2014. A restriction on mean dose to the esophagus < 21 Gy (guideline) or < 34 Gy (limit) was recently described in [35] (“referenced dataset”). In the referenced dataset, the proportion of patients who met the guideline was 40 % and those that met the limit only was 60 %. We assessed the proportion of patients in C1 meeting the guideline (16 % or 37 patients) or the limit only (56 % or 131 patients). To mimic the proportions in the referenced dataset, we included all 37 patients in C1 who met the guideline and a random sample of 24 patients who only met the limit. Treatment plans of the selected patients were rescaled to prescriptions in Table 2. Rescaled plans eligible for the proposed protocol were noted, and for each prescription, the eligible proportion was calculated. Eligibility was estimated in a second cohort (C2) of 21 patients receiving 15 fractions of 4 Gy between 2016 and 2017. The estimated number of patients meeting the eligibility criteria across all prescriptions considered totaled ~272/year.

5. Discussion and conclusion

We developed an open-source platform, ROE, that uses TCP/BED and NTCP models, and dose-volume constraints for interactive, patient-specific prescription optimization. ROE assesses the potential for dose-escalation where possible, without exceeding preset dose-tolerances of normal structures. Otherwise, limiting factors are identified, along with the suggested prescription for safe treatment.

The sample applications described in Section 4 demonstrate that ROE can be used to identify new fractionations that yield higher TCP than conventional schedules without systematic re-planning. Tools in CoROE can be applied to identify (1) the clinical (NTCP/dose-volume) constraints that are hardest to achieve and estimate how often they will materially affect the treatment plan and (2) “problematic” patients, whose TCP could not be improved without violating clinical constraints. It should be noted that assessments of treatments derived from CoROE may be conservative since they (1) do not account for additional improvements to the baseline plans at the scaled prescriptions and (2) are limited by the quality of the baseline plans. Additionally, ROE does not take into account deliverability. We expect that the scaled plan from

ROE will be re-optimized by the treatment planner, at which point the attainability of the final plan using the associated treatment equipment should be assessed.

ROE's library of dosimetric models is currently limited to 14 published DVH-based models applicable across 4 sites (Table 1). Future additions will be documented at [https://github.com/cerr/CERR/wiki/Radiotherapy-Outcomes-Estimator-\(ROE\)](https://github.com/cerr/CERR/wiki/Radiotherapy-Outcomes-Estimator-(ROE)) and available for download along with CERR. However, users are not limited to predefined models as ROE is designed to support custom (user-defined) models, allowing for flexible extension, e.g. the underlying CERR machinery readily supports introducing models based on dose-surface histograms, 2D dose maps, and correlated spatial information such as radiosensitivity maps. Users should bear in mind that all model parameters are treated as fixed, and the interface in its current form does not display confidence intervals associated with TCPs and NTCPs.

ROE provides five of the six desired features for biologically-based treatment planning systems identified by the AAPM therapy physics task group [6]. We intend on meeting the final recommendation by incorporating the ability to balance NTCP/DVH constraints against TCP (currently in ROE) directly into the treatment planning system (e.g. through our prioritized optimization system ECHO [33], by simultaneously optimizing both relative dose distributions and prescription/-fractionation). Future improvements would include the ability to (1) compare outcomes across different treatment plans and (2) display confidence intervals associated with predicted outcomes and (3) support models based on dose-surface histograms, 2D dose maps, and correlated spatial information.

From a clinical perspective, this tool could enable physicians to discuss risks and benefits of a given protocol in a quantitative manner for patient awareness and consent. It could also aid in identifying high-risk patients for intensive outcomes-surveillance programs such as [36]. A prospective protocol to test the feasibility and safety of personalized prescription using CoROE in ultra-central lung cancer patients is currently planned at our institution.

Declaration of Competing Interest

The authors declare that they have no known competing financial interests or personal relationships that could have appeared to influence the work reported in this paper.

Appendix A.1

Mathematical background for the generation of dose-response curves in ROE

A relative dose distribution is first constructed from the input physical dose distribution, D_i with delivered prescription D_p and then rescaled to simulate the desired fractionation scheme with fraction size d_o in N_o fractions.

$$D_a = D_i \cdot d_o \cdot N_o / D_p \quad (1)$$

Note: This only applies to the physical dose (and EQD isodose) plan; the percent isodose plan remains unchanged.

To apply a model distributed with ROE, dose-volume histograms are computed from D_a for the structure(s) of interest, and the resulting dose bins are transformed using the linear quadratic model to match the reference dataset (dose D_b delivered in N_b fractions) used to derive the model.

A scheme delivering dose D_a in N_a fractions is converted to a biologically equivalent scheme delivering dose D_b in N_b fractions following:

$$D_b = \frac{-b \pm \sqrt{b^2 - 4ac}}{2a} \quad (2)$$

Where $a = N_a$, $b = N_a \cdot N_b \cdot \frac{\alpha}{\beta}$ and $c = -D_a(b + D_a N_b)$ and the α/β ratio parameter represents the radiobiological effect of fractionation in the structure of interest.

Alternatively, the Linear Quadratic Model [32] is applied to convert dose D_a with fraction size d_a to an equivalent dose D_b producing the same biological effect when delivered with fraction size d_b :

$$D_b = \frac{D_a \left(d_a + \frac{\alpha}{\beta} \right)}{d_b + \frac{\alpha}{\beta}} \quad (3)$$

Given model parameters Θ , predicted outcomes (P) for the desired baseline fractionation (i.e., at scale factor = 1) are now readily computed from D_b :

$$P_b = f(D_b, \Theta) \quad (4)$$

Dose D_b can further be scaled to estimate outcomes at (i) a range of fraction sizes, keeping fraction number fixed, e.g., for dose $D_{b'} = d_{b'} N_b$

$$P_{b'} = f(k D_b, \Theta) \quad (5)$$

where scale factor $k = d_{b'}/d_b$

(ii) a range of fraction numbers, keeping fraction sizes fixed e.g. for dose $D_{b'} = d_b N_{b'}$

$$P_{b'} = f(k D_b, \Theta) \quad (6)$$

where $N_{b'} = N_b \pm n$ and scale factor $k = (N_b \pm n)/N_b$.

References

- [1] E. Rosenblatt, Planning national radiotherapy services, *Front. Oncol.* 4 (2014) 315.
- [2] H. Enderling, J.C.L. Alfonsi, E. Moros, J.J. Caudell, L.B. Harrison, Integrating mathematical modeling into the roadmap for personalized adaptive radiation therapy, *Trends Cancer* 5 (8) (2019) 467–474.
- [3] B. Sanchez-Nieto, A.E. Nahum, BIOPLAN: software for the biological evaluation of radiotherapy treatment plans, *Med. Dosimetry* 25 (2) (2000) 71–76.
- [4] B. Warkentin, P. Stavrev, N. Stavreva, C. Field, B.G. Fallone, A TCP-NTCP estimation module using DVHs and known radiobiological models and parameter sets, *J. Appl. Clin. Med. Phys.* 5 (1) (2004) 50–63.
- [5] NMILII-BioSuite Team, BioSuite: a comprehensive bioinformatics software package (A unique industry—Academia collaboration), *Curr. Sci.* (2007) 29–38.
- [6] X. Allen Li, M. Alber, J.O. Deasy, A. Jackson, K.W. Ken Jee, L.B. Marks, M. K. Martel, C. Mayo, V. Moiseenko, A.E. Nahum, A. Niemierko, The use and QA of biologically related models for treatment planning: short report of the TG-166 of the therapy physics committee of the AAPM, *Med. Phys.* 39 (3) (2012) 1386–1409.
- [7] J.O. Deasy, A.I. Blanco, V.H. Clark, CERR: a computational environment for radiotherapy research, *Med. Phys.* 30 (5) (2003) 979–985.
- [8] Chen, I., Iyer, A., Thor, M., Wu A.J., M.D., Aptea, Rimnear, A., Gomez D., Deasy, J. O., Jackson, A., 2023. Simulating the potential of model-based individualized prescriptions for ultracentral lung tumors. *Manuscript submitted for publication*.
- [9] Crockford, D., 2006. JSON: the fat-free alternative to XML. <http://www.json.org/xml.html>.
- [10] J.T. Lyman, Complication probability as assessed from dose-volume histograms, *Radiat. Res.* 104 (1985) S13–S19, 2s.
- [11] D.R. Cox, Regression models and life-tables, *J. R. Stat. Soc. Ser. B (Methodol.)* 34 (2) (1972) 187–202.
- [12] M. Roach III, D.M. Chinn, J. Holland, M. Clarke, A pilot survey of sexual function and quality of life following 3D conformal radiotherapy for clinically localized prostate cancer, *Int. J. Rad. Oncol. Biol. Phys.* 35 (5) (1996) 869–874.
- [13] T. Rancati, M. Schwarz, A.M. Allen, F. Feng, A. Popovtzer, B. Mittal, A. Eisbruch, Radiation dose–volume effects in the larynx and pharynx, *Int. J. Rad. Oncol. Biol. Phys.* 76 (3) (2010) S64–S69.
- [14] E.X. Huang, A.J. Hope, P.E. Lindsay, M. Trovo, I. El Naqa, J.O. Deasy, J.D. Bradley, Heart irradiation as a risk factor for radiation pneumonitis, *Acta Oncol. (Madr)* 50 (1) (2011) 51–60.
- [15] R. Wijsman, F. Dankers, E.G. Troost, A.L. Hoffmann, E.H. Van Der Heijden, L.F. de Geus-Oei, J. Bussink, Multivariable normal-tissue complication modeling of acute esophageal toxicity in advanced stage non-small cell lung cancer patients treated with intensity-modulated (chemo-) radiotherapy, *Radiotherapy Oncol.* 117 (1) (2015) 49–54.
- [16] A. Fontanella, C. Robinson, A. Zuniga, A. Apte, W. Thorstad, J. Bradley, J. Deasy, SU-E-T-312: test of the Generalized Tumor Dose (gTD) model with an independent lung tumor dataset, *Med. Phys.* 41 (6Part16) (2014) 296. –296.
- [17] H. Tekatli, M. Duijm, E. Oomen-de Hoop, W. Verbakel, W. Schillemans, B. J. Slotman, J.J. Nuyttens, S. Senan, Normal tissue complication probability modeling of pulmonary toxicity after stereotactic and hypofractionated radiation therapy for central lung tumors, *Int. J. Rad. Oncol. Biol. Phys.* 100 (3) (2018) 738–747.
- [18] M. Thor, J.O. Deasy, A. Iyer, E. Bendau, A. Fontanella, A. Apte, E. Yorke, A. Rimner, A. Jackson, Toward personalized dose-prescription in locally advanced non-small cell lung cancer: validation of published normal tissue complication probability models, *Radiotherapy. Oncol.* 138 (2019) 45–51.
- [19] I. Chen, A.J. Wu, A. Jackson, P. Patel, L. Sun, A. Ng, A. Iyer, A. Apte, A. Rimner, D. Gomez, J.O. Deasy, External validation of pulmonary radiotherapy toxicity models for ultracentral lung tumors, *Clin. Transl. Rad. Oncol.* 38 (2023) 57–61.
- [20] J.M. Michalski, H. Gay, A. Jackson, S.L. Tucker, J.O. Deasy, Radiation dose–volume effects in radiation-induced rectal injury, *Int. J. Rad. Oncol. Biol. Phys.* 76 (3) (2010) S123–S129.
- [21] M.R. Cheung, S.L. Tucker, L. Dong, R. De Crevoisier, A.K. Lee, S. Frank, R. J. Kudchadker, H. Thames, R. Mohan, D. Kuban, Investigation of bladder dose and volume factors influencing late urinary toxicity after external beam radiotherapy for prostate cancer, *Int. J. Radiat. Oncol. Biol. Phys.* 67 (4) (2007) 1059–1065.
- [22] T.P. Kole, B. Wu, M. Tong, S. Lei, L.N. Chen, S. Suy, A. Dritschilo, E.D. Yorke, S. P. Collins, Late urinary toxicity modeling after stereotactic body radiation therapy (SBRT) in the definitive treatment of localized prostate cancer, *Int. J. Radiat. Oncol. Biol. Phys.* 90 (1) (2014) S53–S54.
- [23] C.C. Pan, B.D. Kavanagh, L.A. Dawson, X.A. Li, S.K. Das, M. Miften, R.K. Ten Haken, Radiation-associated liver injury, *Int. J. Rad. Oncol. Biol. Phys.* 76 (3) (2010) S94–S100.
- [24] M. Thor, J.O. Deasy, C. Hu, E. Gore, V. Bar-Ad, C. Robinson, M. Wheatley, J.H. Oh, J. Bogart, Y.I. Garces, V.S. Kavadi, Modeling the impact of cardiopulmonary irradiation on overall survival in NRG oncology trial RTOG 0617, *Clin. Cancer Res.* 26 (17) (2020) 4643–4650.
- [25] K.C. Chao, J.O. Deasy, J. Markman, J. Haynie, C.A. Perez, J.A. Purdy, D.A. Low, A prospective study of salivary function sparing in patients with head-and-neck cancers receiving intensity-modulated or three-dimensional radiation therapy: initial results, *Int. J. Rad. Oncol. Biol. Phys.* 49 (4) (2001) 907–916.
- [26] J.F. Fowler, Biological factors influencing optimum fractionation in radiation therapy, *Acta Oncol. (Madr)* 40 (6) (2001) 712–717.
- [27] J. Jeong, J. Oh, A. Fontanella, M. Crispin-Ortuzar, J.O. Deasy, Comparison between mechanistic radiobiological modeling vs. fowler BED equation in evaluating lung cancer radiotherapy outcome for a broad range of fractionation, *Med. Phys.* 4 (6) (2017).
- [28] J. Jeong, J.H. Oh, J.J. Sonke, J. Belderbos, J.D. Bradley, A.N. Fontanella, S.S. Rao, J.O. Deasy, Modeling the cellular response of lung cancer to radiation therapy for a broad range of fractionation schedules, *Clin. Cancer Res.* 23 (18) (2017) 5469–5479.
- [29] S. Walsh, E. Roelofs, P. Kuess, P. Lambin, B. Jones, D. Georg, F. Verhaegen, A validated tumor control probability model based on a meta-analysis of low, intermediate, and high-risk prostate cancer patients treated by photon, proton, or carbon-ion radiotherapy, *Med. Phys.* 43 (2) (2016) 734–747.
- [30] A.L. Appelt, I.R. Vogelius, K.P. Farr, A.A. Khalil, S.M. Bentzen, Towards individualized dose constraints: adjusting the QUANTEC radiation pneumonitis model for clinical risk factors, *Acta Oncol. (Madr)* 53 (5) (2014) 605–612.
- [31] S.U. Din, E.L. Williams, A. Jackson, K.E. Rosenzweig, A.J. Wu, A. Foster, E. D. Yorke, A. Rimner, Impact of fractionation and dose in a multivariate model for radiation-induced chest wall pain, *Int. J. Radiat. Oncol. Biol. Phys.* 93 (2) (2015) 418–424.
- [32] B.G. Douglas, J.F. Fowler, Fractionation schedules and a quadratic dose-effect relationship, *Br. J. Radiol.* 48 (570) (1975) 502–503.
- [33] M. Zarepisheh, L. Hong, Y. Zhou, J.H. Oh, J.G. Mechala, M.A. Hunt, G. S. Mageras, J.O. Deasy, Automated intensity modulated treatment planning: the expedited constrained hierarchical optimization (ECHO) system, *Med. Phys.* 46 (7) (2019) 2944–2954.
- [34] D.R. Gomez, S.L. Tucker, M.K. Martel, R. Mohan, P.A. Balter, J.L. Guerra, H. Liu, R. Komaki, J.D. Cox, Z. Liao, Predictors of high-grade esophagitis after definitive three-dimensional conformal therapy, intensity-modulated radiation therapy, or proton beam therapy for non-small cell lung cancer, *Int. J. Rad. Oncol. Biol. Phys.* 84 (4) (2012) 1010–1016.
- [35] E.D. Yorke, M. Thor, D.Y. Gelblum, D.R. Gomez, A. Rimner, N. Shaverdian, A. F. Shepherd, C.B. Simone, A. Wu, D. McKnight, A. Jackson, Treatment planning and outcomes effects of reducing the preferred mean esophagus dose for conventionally fractionated non-small cell lung cancer radiotherapy, *J. Appl. Clin. Med. Phys.* 22 (2) (2021) 42–48.
- [36] M. Thor, E.D. Yorke, J.M. Moran, B. Daly, D.R. Gomez, J.O. Deasy, PO-1250 Exploring published acute esophagitis models to support improved clinical management in thoracic RT, *Radiotherapy Oncol.* 170 (2022) S1054–S1055.